Bioconjugate Chemistry

Article

pubs.acs.org/bc

1,2,3-Triazole Stabilized Neurotensin-Based Radiopeptidomimetics for Improved Tumor Targeting

Alba Mascarin, Ibai E. Valverde, Sandra Vomstein, and Thomas L. Mindt*

Division of Radiopharmaceutical Chemistry, University of Basel Hospital, Petersgraben 4, 4031 Basel, Switzerland

Supporting Information

ABSTRACT: Neurotensin (NT) is a regulatory peptide with nanomolar affinity toward NT receptors, which are overexpressed by different clinically relevant tumors. Its binding sequence, NT(8−13), represents a promising vector for the development of peptidic radiotracers for tumor imaging and therapy. The main drawback of the peptide is its short biological half-life due to rapid proteolysis *in vivo*. Herein, we present an innovative strategy for the stabilization of peptides using nonhydrolizable 1,4-disubstituted, 1,2,3-triazoles as amide bond surrogates. A "triazole scan" of the peptide sequence yielded novel NT(8−13) analogues with enhanced stability, retained receptor affinity, and improved tumor targeting properties *in vivo*. The synthesis of libraries of triazole-based peptidomimetics was achieved efficiently on solid support by a combination of Fmoc-peptide chemistry, diazo transfer reactions, and the Cu(I)-catalyzed alkyne azide cycloaddition (CuAAC) employing methods that are fully compatible with standard solid phase peptide synthesis (SPPS) chemistry. Thus, the amide-to-triazole substitution strategy may represent a general methodology for the metabolic stabilization of biologically active peptides.

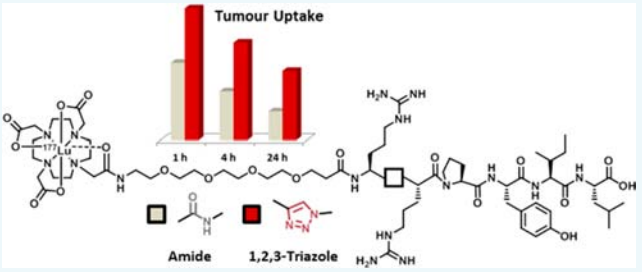

INTRODUCTION

Neurotensin (NT) is a 13 amino acid regulatory peptide, naturally present in the human body. It is localized in the central nervous system as well as in peripheral tissues, especially in the gastrointestinal tract, and it has the function of a neurotransmitter and neuromodulator.[1,2] It was first isolated from bovine hypothalami by Carraway and Leeman in 1973.[1] Three main NT receptors (NTR1, NTR2, and NTR3) have been identified so far in mammals. A fourth (NTR4) has been identified in bullfrogs.[3] NTR1, NTR2, and NTR4 belong to the G-protein coupled receptors (GPCR), whereas NTR3 is a member of the Vps10p domain receptor family and possesses a single transmembrane domain.[4] The natural ligand, NT, has both a high specificity and affinity to these receptors.[4] The most interesting receptor, NTR1, is overexpressed in various clinically relevant tumors, such as Ewing's sarcoma,[5] ductal breast cancer,[6] and exocrine pancreatic tumors.[7] Seventy-five percent of ductal pancreatic adenocarcinomas express NTR1 receptors in high incidence.[7] This type of cancer has a high occurrence in Western countries and is very aggressive, and due to a lack of diagnostic tools, an early diagnosis is currently not possible. Consequently, NT and derivatives of its minimal binding sequence NT(8−13) (Arg^8-Arg^9-Pro^{10}-Tyr^{11}-Ile^{12}-Leu^{13})[8] represent promising tumor targeting vectors for the development of new diagnostic and therapeutic agents, e.g., radiopharmaceuticals.

A drawback of NT(8−13) is its inherent low stability *in vivo*. It is rapidly degraded by the endogenous proteases present in blood serum, resulting in a biological half-life of only a few minutes.[9] Metalloendopeptidases 24.15 and 24.16 are responsible for the cleavage of the Arg^8-Arg^9 and Pro^{10}-Tyr^{11} bonds,[10] while the Angiotensin-converting enzyme 15.1 and endopeptidase 24.11 are involved in the hydrolysis of the Pro^{10}-Tyr^{11} and Tyr^{11}-Ile^{12} bonds. Several peptide stabilization techniques have been applied to NT including the reduction or *N*-methylation of amide bonds,[11,12] amino acid substitution with, e.g., D- and other noncanonical amino acids,[12−14] and the formation of multimeric NT conjugates,[15,16] however, with varying degree of success. Despite considerable research efforts in the past years, only one example of a radiolabeled NT derivative has been evaluated in a clinical trial.[17]

For these reasons, we are interested in the development of new approaches for the metabolic stabilization of tumor-targeting peptides, in particular NT. Specifically, we are investigating the utility of 1,4-disubstituted 1,2,3-triazoles as metabolically stable *trans*-amide bond mimics. 1,2,3-Triazoles have been described in the literature as amide bond bioisosters,[18−23] as they are similar in terms of size, planarity, hydrogen bonding properties, and dipole moment. However, examples of their application for the stabilization of linear peptides with high receptor affinity remain scarce.[24,25] We have previously demonstrated the potential of the amide-to-triazole substitution strategy with derivatives of the tumor-targeting peptide Bombesin. The systematic replacement of single amide bonds by the 1,2,3-triazole heterocycle in the backbone of the peptide, termed a "triazole scan", provided several stabilized

Received: August 8, 2015
Revised: September 4, 2015
Published: September 8, 2015

DOI: 10.1021/acs.bioconjchem.5b00444
Bioconjugate Chem. 2015, 26, 2143−2152

radiolabeled peptidomimetics with improved tumor-targeting properties *in vivo*.[24] As a continuation of our ongoing research program, we report here the first triazole scan of NT(8−13). The NT-derived peptidomimetics obtained were radiolabeled with ^{177}Lu via the chelator 1,4,7,10-tetraazacylododecane-1,4,7,10-tetraacetic acid (DOTA) conjugated to the *N*-terminus of the peptide through a tetraethylene glycol (PEG_4) spacer (see below). After the identification of the amide bonds of the original amino acid sequence amenable for the modification, we applied the same methodology to a second generation of triazole-modified NT(8−13) analogues in which Ile[12] was exchanged to Tle[12],[12,26] a strategy reported for the stabilization of the peptide. All triazole containing compounds with retained nanomolar affinity to NTR1 and improved stability were fully evaluated *in vitro* and *in vivo* and compared side-by-side with the corresponding unmodified (all amide bond) reference compounds.

RESULTS AND DISCUSSION

Syntheses and Radiolabeling. Access to 1,2,3-triazole modified peptidomimetics requires the corresponding amino acid-derived alkyne building blocks. α-Amino alkynes were prepared by adapted procedures reported in the literature (Scheme 1). In brief, Weinreb amides of amino acids were reduced with DIBAL-H to the corresponding α-amino aldehydes, which were then subjected *in situ* to a Seyferth-Gilbert homologation,[27] using the Bestmann-Ohira reagent.[28] For amino acids without a functional group in the side chain, the respective Boc-protected starting materials were employed (Route A). However, Fmoc-protected precursors were used for substrates bearing orthogonally protected functional groups in their side chains (Route B). In this case, a mixture of the corresponding α-amino protected/deprotected products was obtained, which was conveniently converted to the desired Fmoc-derivatives by treatment of the crude product mixtures with Fmoc-OSu. All α-amino alkynes were obtained in good to satisfying yields. To verify the enantiomeric purity of the compounds, they were subjected to α-amino deprotection and coupling with Fmoc-Ala-OH followed by determination of the diastereomeric purity of the pseudodipeptides by NMR spectroscopy (Supporting Information). In neither case was a racemization observed. So far, we have investigated 11 alkyne derivatives of the approximately 20 natural α-amino acids (Ala, Arg, Gly, Gln, Ile, His, Leu, Pro, Trp, Tyr, and Val), and only in the case of His was a partial racemization (<20%) observed.[24]

Scheme 1. Synthesis of α-Amino Alkynes[a]

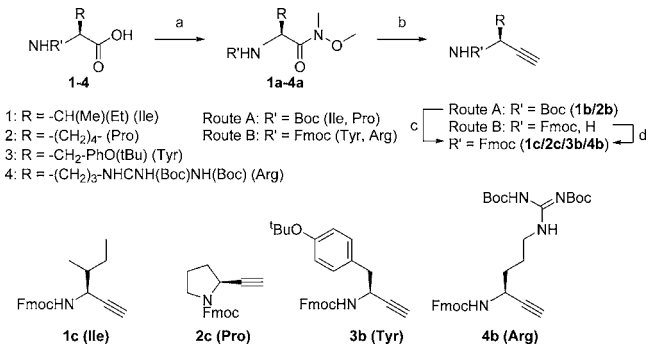

[a](a) For Ile, Tyr, and Pro: DIPEA, BOP, *N*,*O*-dimethylhydroxylamine, CH_2Cl_2, 12 h, rt. For Arg: HOBT, EDC, *N*-methylmorpholine, *N*,*O*-dimethylhydroxylamine, CH_2Cl_2, 12 h, rt; (b) (i) DIBAL-H, CH_2Cl_2, 2 h, −78°C; (ii) Bestmann-Ohira reagent, K_2CO_3, MeOH, 0 °C; then 12 h, rt; (c) (i) 20% TFA in CH_2Cl_2, 30 min, rt; (ii) Fmoc-OSu, DIPEA, 2 h, rt; (d) Fmoc-OSu, DIPEA, 2 h, rt. For Ile **1c** and Pro **2c** see also the literature reference.[29].

With the α-amino alkyne derivatives in hand, we next went on with the synthesis of peptidomimetics on solid support. In general, the peptides were built up on a Fmoc-Leu preloaded resin by standard Fmoc SPPS up to the amide bond position to be replaced by a 1,2,3-triazole. At this stage, the *N*-terminal amine of the peptide was deprotected and converted to an azide by a diazo transfer reaction using the reagent imidazolyl-1-sulfonyl azide.[30,31] The copper(I)-catalyzed azide−alkyne cycloaddtion (CuAAC; click chemistry)[18,32] was then performed with the resin-bound azide and the corresponding Fmoc-protected α-amino alkyne derivative using $[(CH_3CN)_4Cu]PF_6$ as a copper(I) source and DIPEA as a base. After the insertion of the 1,2,3-triazole heterocycle, the peptide sequence was completed by SPPS and elongated *N*-terminally with a short hydrophilic tetraethylene glycol (PEG_4) spacer for optimizing the biological properties of the final conjugate[33] and the universal macrocyclic chelator DOTA which allows for the radiolabeling with different metallic radionuclides. The synthesis of triazole-containing peptide conjugates is illustrated in Scheme 2 by the example of **NT VI**. The preparation of the NT-derivative with a *C*-terminal, monosubstituted 1,2,3-triazole (**NT II**) was accomplished following previously published procedures as was the *N*-terminal modification (**NT VII**) using an alkyne derivative of the PEG_4 spacer.[24] After completion of the synthesis, the peptide conjugates were cleaved from the resin, deprotected, and purified by preparative HPLC. All compounds were obtained in good to satisfying overall yields, and their structures were confirmed by mass spectrometry (Table 1).

In the first series, we performed a triazole scan of NT(8−13) which included the systematic replacement of each amide bond of the peptide, one at the time, but between Arg[9]-Pro[10] due to the secondary amine of Pro which does not allow for the introduction of an azide functionality. The triazole scan provided NT conjugates **NT II**−**VII** (Table 1) along with reference compound **NT I**. After identification of the positions that tolerate an amide-to-triazole substitution (*N*-terminus and between the residues Arg[9]-Arg[8]), a second generation of NT-based peptidomimetics was prepared (**NT VIII-X**). This included, in addition to the triazole insertion into the backbone of the peptide, a variation of the amino acid sequence by an Ile[12]-to-Tle[12] switch. The latter modification has been reported as a successful stabilization strategy of the peptide.[12,26,34,35]

Neurotensin analogues **NT I-X** were radiolabeled with $[^{177}Lu]LuCl_3$ according to established procedures in NH_4OAc (400 mM, pH 5.0) at 95 °C for 30 min yielding the corresponding radiometalated conjugates [^{177}**Lu**]-**NT I-X** in high radiochemical yields and purities exceeding >95% (Supporting Information).[24] Specific activities ranged from 5 to 43 MBq/nmol (not optimized). Lu-177 was selected as a radionuclide for this study because it is a therapeutic β^--particle emitter with a concomitant γ-radiation, which makes it an interesting radionuclide for theranostic applications.[36] All radiolabeled derivatives were subjected to evaluations of their biological properties.

***In Vitro* Evaluations.** The cell internalization properties and receptor affinities (K_D) of ^{177}Lu-labeled NT-derivatives were evaluated *in vitro* with NTR1-expressing HT-29 cells

DOI: 10.1021/acs.bioconjchem.5b00444
Bioconjugate Chem. 2015, 26, 2143−2152

Scheme 2. Example of the Synthesis of a Radiolabeled Triazole-Backbone Modified NT(8-13) Conjugate ([^{177}Lu]-NT VI)[a]

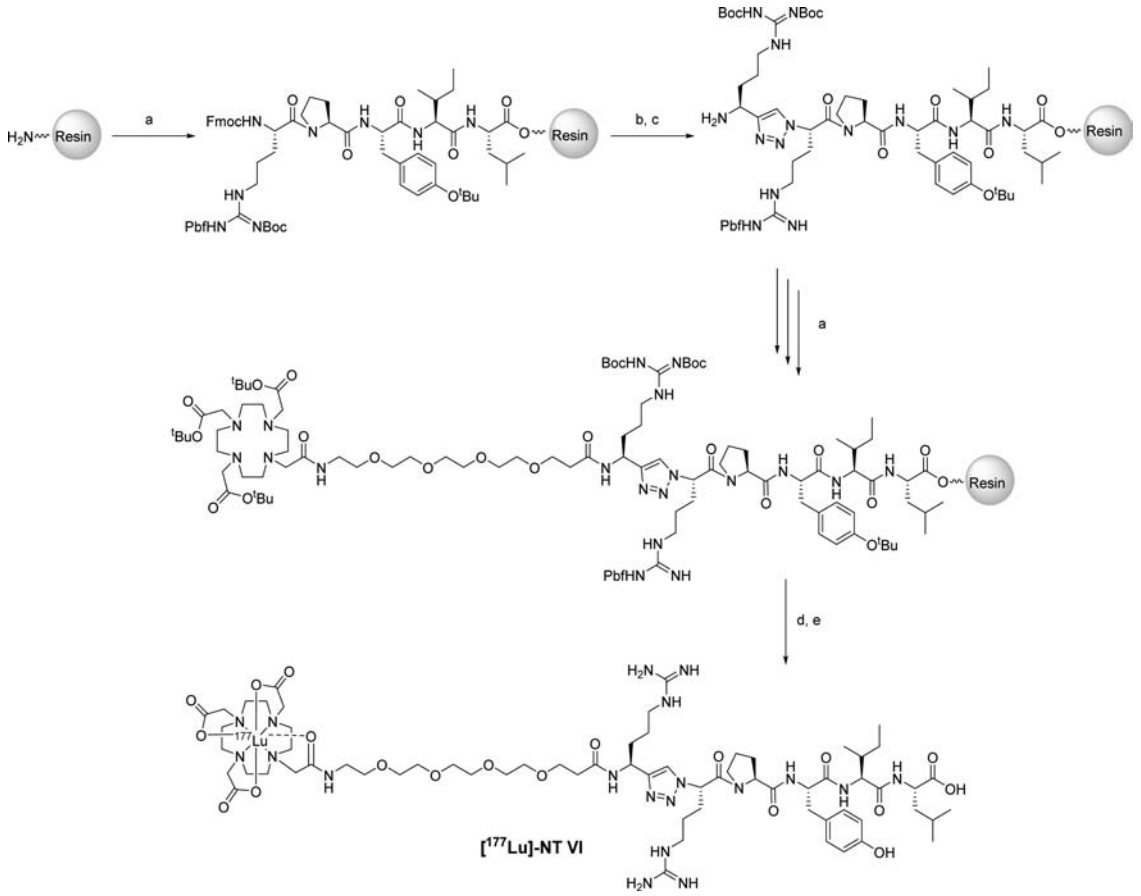

[a](a) Fmoc SPPS: (1) 20% piperidine in DMF, rt; (2) Fmoc-amino acid, Fmoc-PEG$_4$-H, or DOTA-(tris-^{t}Bu); HATU, DIPEA, DMF, 2 h, rt; (b) solid phase azide formation: imidazole-1-sulfonyl hydrochloride, DIPEA, DMF, 1 h, rt; (c) solid phase CuAAC; Fmoc-alkyne, [Cu(CH$_3$CN)$_4$]PF$_6$, TBTA, DIPEA, DMF, 12 h, rt; (d) TFA/H$_2$O/PhOH/*i*Pr$_3$SiH, 6 h, rt; (e) [^{177}Lu]LuCl$_3$, NH$_4$OAc (pH 5.0), 30 min, 100 °C.

Table 1. Structures and ESI-MS Data of Peptide Conjugates NT I-X

compound	structure[a]	M_W calcd.	$[M + 2H^+]^{2+}$ observed
NT I	DOTA-PEG$_4$-Arg-Arg-Pro-Tyr-Ile-Leu	1449.82	725.92
NT II	DOTA-PEG$_4$-Arg-Arg-Pro-Tyr-Ile-Leu-**ψ[Tz]-H**	1473.85	737.92
NT III	DOTA-PEG$_4$-Arg-Arg-Pro-Tyr-Ile-**ψ[Tz]**-Leu	1473.83	738.92
NT IV	DOTA-PEG$_4$-Arg-Arg-Pro-Tyr-**ψ[Tz]**-Ile-Leu	1473.83	737.92
NT V	DOTA-PEG$_4$-Arg-Arg-Pro-**ψ[Tz]**-Tyr-Ile-Leu	1473.83	737.92
NT VI	DOTA-PEG$_4$-Arg-**ψ[Tz]**-Arg-Pro-Tyr-Ile-Leu	1473.83	737.92
NT VII	DOTA-PEG$_4$-**ψ[Tz]**-Arg-Arg-Pro-Tyr-Ile-Leu	1459.81	730.92
NT VIII	DOTA-PEG$_4$-Arg-Arg-Pro-Tyr-**Tle**-Leu	1449.92	725.92
NT IX	DOTA-PEG$_4$-Arg-**ψ[Tz]**-Arg-Pro-Tyr-Tle-Leu	1473.83	737.92
NT X	DOTA-PEG$_4$-**ψ[Tz]**-Arg-Arg-Pro-Tyr-Tle-Leu	1459.81	730.91

[a]ψ[Tz] represents the replacement of an amide bond by a 1,4-disubstituted [1,2,3]-triazole.

(colon carcinoma cells) and compared side-by-side with the unmodified (all amide bond) reference compounds. The specificity of radiotracers with retained receptor affinity toward NTR1 was verified by blocking experiments. In each case, the presence of 1000-fold excess NT(8−13) resulted in a decrease of cell-associated radioactivity to less than approximately 0.3% (see Supporting Information).

Reference compound [^{177}**Lu**]-**NT I** for the first generation of peptidomimetics obtained from the triazole scan (**NT II**−**VII**) exhibited a cell internalization of 7.3% after 4 h and a single-digit nanomolar binding affinity toward NTR1 (Table 2), which is in agreement with literature data reported for related NT-based radiotracers.[37] Disappointingly, compounds [^{177}**Lu**]-**NT II**−**V** did not bind to HT-29 cells; however, radioconjugates [^{177}**Lu**]-**NT VI** and **VII** with a triazole introduced in the *N*-terminal region of the peptide showed *in vitro* properties similar to those of the reference compound in terms of cell internalization and K_D. These results can be explained based on recently published X-ray crystallographic data of NT(8−13) bound to NTR1, which show that the *C*-terminal and central regions of the ligand are involved in several hydrogen bonding interactions to residues of the receptor, whereas the *N*-terminus of the peptide is pointing out of the binding pocket.[38] These findings provide a rationale of the results of our work and those

DOI: 10.1021/acs.bioconjchem.5b00444
Bioconjugate Chem. 2015, 26, 2143−2152

Table 2. *In Vitro* Properties of the Radiolabeled Compounds [^{177}Lu]-NT I-X

compound	cell uptake [%] after 4 h[a,b]	K_D [nM][b,d]	stability after 4 h [%][e] ($t_{1/2}$ in min)[f]
[^{177}Lu]-NT I	7.3 ± 0.4	3.7 ± 0.8	0.9 ± 0.3 (39.4)
[^{177}Lu]-NT II	n.o.[c]	n.d.	21.3 ± 1.8 (69.7)
[^{177}Lu]-NT III	n.o.[c]	n.d.	30.0 ± 3.6 (72.0)
[^{177}Lu]-NT IV	n.o.[c]	n.d.	46.1 ± 3.8 (164.0)
[^{177}Lu]-NT V	n.o.[c]	n.d.	0 (13.0)
[^{177}Lu]-NT VI	6.4 ± 1.2	8.8 ± 1.7	6.5 ± 4.6 (64.9)
[^{177}Lu]-NT VII	9.4 ± 0.5	4.5 ± 0.8	2.2 ± 1.2 (46.9)
[^{177}Lu]-NT VIII	1.3 ± 0.2	507 ± 114	70.6 ± 1.4 (n.d.)
[^{177}Lu]-NT IX	2.1 ± 0.1	214 ± 45	97.7 ± 2.3 (n.d.)
[^{177}Lu]-NT X	1.2 ± 0.2	>1000	94.7 ± 4.2 (n.d.)

[a]Receptor specific cell-bound and internalized fraction of compounds expressed in % of administered dose normalized to 10^6 cells. [b]The values given are the means with standard deviations of at least two experiments performed in triplicate (n = 2−3). [c]n.o: not observed; no specific binding or internalization was detected at a peptide concentration of 2.5 pmol/well. [d]Determined by receptor saturation binding assay. [e]Determined in blood serum at 37 °C, expressed in % of intact peptide after 4 h of incubation. [f]Calculated biological half-life in minutes, by fitting the data ($n \geq 2-3$) with the equation $A_{(t)} = A_0 \cdot \exp(-\lambda \cdot t)$ (Prism 5.0). n.d.: not determined.

of others in that structural modifications of NT(8−13) are only tolerated at its *N*-terminus.[11,39]

Next, we studied the effect of the amide-to-triazole substitution on the proteolytic stability of the conjugates. Thus, [^{177}Lu]-**NT I−VII** were incubated in human blood serum, and samples were analyzed at different time-points by γ-HPLC (see Experimental Procedures). In general, the triazole-containing radiolabeled peptide conjugates, including conjugates [^{177}Lu]-**NT VI** and **VII** with retained receptor affinity, exhibited an improved serum stability in comparison to that of reference compound [^{177}Lu]-**NT I** (Table 2 and Figure 1).

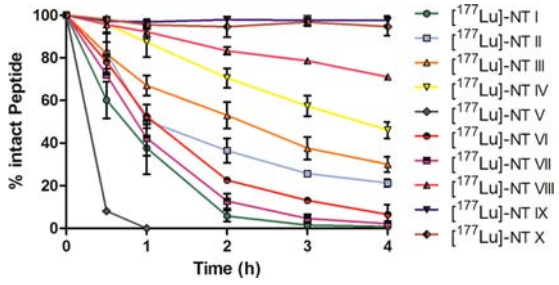

Figure 1. Metabolic stabilities of radiolabeled compounds in human blood serum (30 pmol/mL, 1 nM) expressed as a percentage of intact peptides ($n \geq 2-3$); error bars indicate the standard deviations of mean values.

The *in vitro* studies of [^{177}Lu]-**NT I−VII** indicated that modifications in the vicinity of position Ile^{12} had the most pronounced effect on the stability of the peptide; however, the insertion of a triazole heterocycle as an amide bond mimic at this position proved to be not suitable as indicated by the abolished receptor affinity of compounds [^{177}Lu]-**NT III** and **IV**. For the development of a second generation of stabilized NT-based radiotracers, we thus focused on NT(8−13) derivatives in which Ile^{12} is replaced by a Tle^{12} and applied our amide-to-triazole substitution strategy at positions identified to tolerate such a modification (*N*-terminus and between Arg^8-Arg^9).[12,26,34,35] *In vitro* evaluation of [^{177}Lu]-**NT VIII**, which served as the reference compound for the second generation of NT-based radiotracers (**NT VIII-X**), indicated that the Ile^{12}-to-Tle^{12} switch itself resulted in a significant reduction of cell internalization rates in comparison to those of the Ile^{12}-analogeous compound **NT I** (Figure 2, Table 2). This

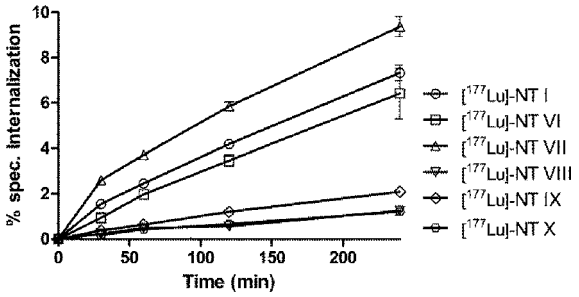

Figure 2. Cell internalization profile of the radiolabeled compounds (2.5 pmol/well, 2.5 pM)) into human colon carcinoma HT-29 cells. Receptor specific cell bound and internalized fraction of compounds is expressed in % of administered dose normalized to 10^6 cells. The experiments were performed in triplicate (n = 2−3); error bars indicate the standard deviations of mean values. Curves of [^{177}Lu]-**NT VIII** and **X** are overlapping.

is likely due to its significantly decreased affinity toward NTR1 as determined by receptor saturation experiments (Figure 3 and

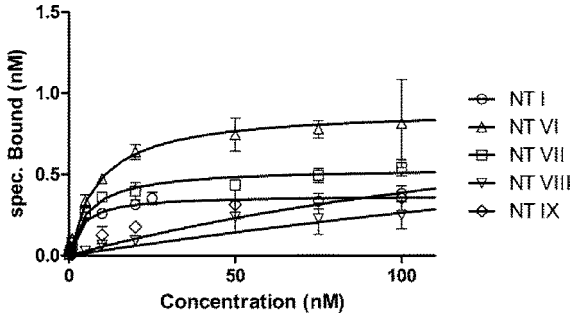

Figure 3. Receptor binding saturation curves of the radiolabeled compounds using human colon carcinoma HT-29 cells. The experiments were performed in triplicate (n = 2−3); error bars indicate the standard deviations of mean values. Different concentrations of the radiotracers were used depending on their receptor affinities (see Experimental Procedures and Supporting Information).

Table 2). However, a remarkable gain with regard to serum stability was observed at the same time (Figure 1 and Table 2); >70% of [^{177}Lu]-**NT VIII** was still intact after 4 h of incubation in serum, a period of time after which all of the first generation Ile^{12} derivatives ([^{177}Lu]-**NT II−VII**) were found metabolized to >50%. Likewise, triazole-containing compounds [^{177}Lu]-**NT IX** and **X** showed the same trend and even a further improved stability as the result of the insertion of a triazole; however, only derivative [^{177}Lu]-**NT IX** retained a submicromolar affinity toward NTR1.

***In Vivo* Evaluations.** Triazole-containing NT(8−13) radioconjugates with retained nanomolar affinities toward the NTR1 and an increased serum stability ([^{177}Lu]-**NT VI**, **VII**, and **IX**) were further evaluated *in vivo* and compared side-by-side with the corresponding reference compounds ([^{177}Lu]-**NT I** and **VIII**, respectively). Biodistribution studies were performed with athymic nude Foxn1^{nu} mice bearing HT-29 xenografts on their

DOI: 10.1021/acs.bioconjchem.5b00444
Bioconjugate Chem. 2015, 26, 2143−2152

right shoulder (n = 4−5 per time point) at 1, 4, and 24 h postinjection (p.i.) of the radiotracers (Figure 4; only a selection of organs is shown; for details, see the Supporting Information). Receptor specificity of the radiotracers was confirmed by blocking experiments 1 h p.i. (n = 3). In each case, the coinjection of 6000-fold excess NT(1−13) resulted in a significant decrease (up to 20-fold) of radioactivity accumulated in receptor positive organs and tumor xenografts (see the Supporting Information).

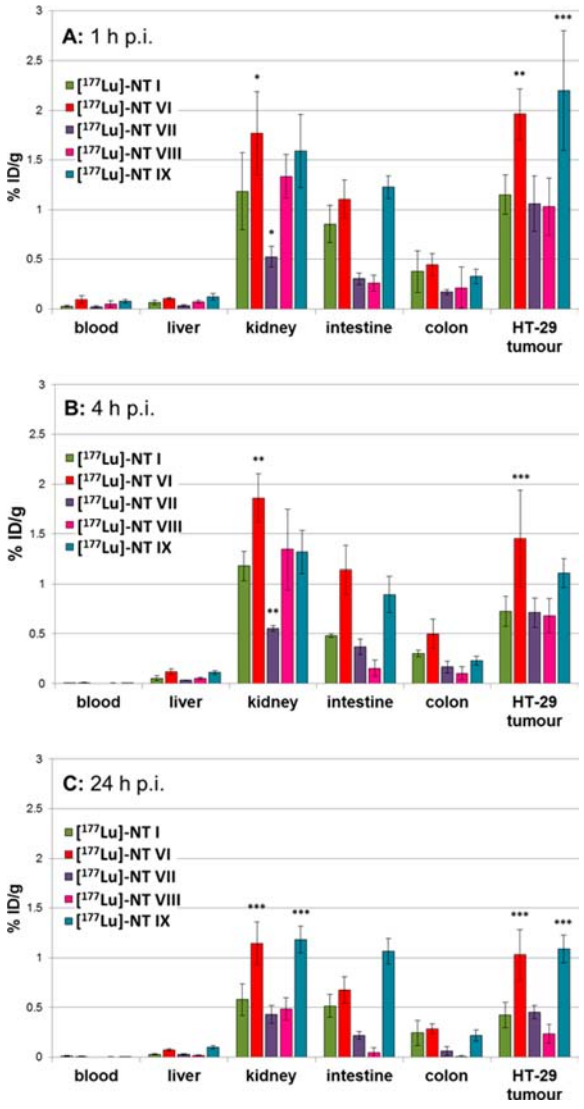

Figure 4. Biodistribution data in nude mice bearing HT-29 tumor xenografts (n = 4−5) at different time points (A, 1 h p.i.; B, 4 h p.i.; C, 12 h p.i.) after intravenous injection of radiolabeled compounds. Results are expressed as % of injected dose per gram of tissue (% ID/g): error bars indicate standard deviations of mean values. Only selected organs are shown (see Supporting Information for details and results of blocking experiments). Statistical significance was determined with a one-way ANOVA and Dunnett's multiple test (* $P < 0.05$; ** $P < 0.01$; ***$P < 0.001$). [^{177}**Lu**]-**NT VI** and [^{177}**Lu**]-**NT VII** were compared to [^{177}**Lu**]-**NT I** and [^{177}**Lu**]-**NT IX** to [^{177}**Lu**]-**NT VIII**.

In general, the investigated radiopeptides and radiopeptidomimetics exhibited a pharmacokinetic profile, which is commonly observed for this class of radiotracers. No or only very low accumulation of radioactivity was observed in receptor negative tissue and organs (e.g., bones, heart, lungs, or liver) resulting in a favorable high signal-to-background ratio. The low levels of radioactivity in the blood and the liver indicate fast blood clearance and the absence of hepatobiliary excretion of the radiotracers and/or their metabolites. Unspecific uptake of radioactivity in the kidneys is the result of renal excretion, a typical characteristic of radiolabeled peptides.

Specific uptake of radiolabeled NT(8−13) derivatives was observed in receptor positive organs (e.g., the colon and intestine) and the tumor xenografts which was followed by a slow wash-out of radioactivity over time; for example, 23−53% of the initially accumulated radioactivity remained in the tumor xenografts after 24 h. These observations are in agreement with data published on related radiolabeled Neurotensin derivatives.[9,12,13,34,35,40] Strikingly, tumor uptake of triazole-stabilized [^{177}**Lu**]-**NT VI** and **IX** was increased up to 2-fold (approximately 2% injected dose (ID)/g) in comparison to that of the corresponding reference compounds [^{177}**Lu**]-**NT I** and **VIII**, respectively (each approximately 1% ID/g). These results suggest that the introduction of a 1,2,3-triazole moiety between the Arg^9-Arg^8 residues of NT(8−13) may represent a general approach to improve the tumor targeting properties of the peptide. Interestingly, both [^{177}**Lu**]-**NT VI** and **IX** had a similar tumor uptake despite their different affinities toward NTR1 (Table 2), an observation which could be ascribed to the significantly improved stability of the latter. Despite its moderate tumor uptake, [^{177}**Lu**]-**NT VII** displayed a high tumor-to-background, in particular tumor-to-kidney ratio (Table 3) at early time points. This is an important characteristic for potential imaging applications of the radiopeptide. Thus, [^{177}**Lu**]-**NT VI** and **IX** may represent interesting candidates for the development of NT-based radiotherapeutics (or theranostics), whereas [^{177}**Lu**]-**NT VII** exhibits promising properties as a diagnostic probe for the imaging of NTR1 expressing tumors. Further optimization of the compounds for potential clinical applications is currently ongoing.

CONCLUSIONS

We have successfully applied our recently developed amide-to-triazole substitution strategy ("triazole scan")[24,49] to the minimal binding sequence of Neurotensin, NT(8−13). The

Table 3. Tumor-to-Background Ratios of Radiolabeled NT-Conjugates at Early Time Points p.i.

	tumor-to-kidney		tumor-to-intestines		tumor-to-colon	
	1 h	4 h	1 h	4 h	1 h	4 h
[^{177}**Lu**]-**NT I**	1.0 ± 0.5	0.6 ± 0.2	1.3 ± 0.5	1.5 ± 0.4	3.1 ± 2.2	2.4 ± 0.8
[^{177}**Lu**]-**NT VI**	1.1 ± 0.4	0.8 ± 0.4	1.8 ± 0.5	1.3 ± 0.7	4.4 ± 1.7	2.9 ± 1.8
[^{177}**Lu**]-**NT VII**	2.0 ± 0.6	1.3 ± 0.3	3.4 ± 1.6	1.9 ± 0.8	6.1 ± 2.5	4.3 ± 2.4
[^{177}**Lu**]-**NT VIII**	0.8 ± 0.3	0.5 ± 0.3	4.0 ± 6.0	4.5 ± 3.5	4.8 ± 6.0	6.6 ± 5.8
[^{177}**Lu**]-**NT IX**	1.4 ± 0.7	0.8 ± 0.2	1.8 ± 0.7	1.2 ± 0.4	6.7 ± 3.3	4.9 ± 1.6

DOI: 10.1021/acs.bioconjchem.5b00444
Bioconjugate Chem. 2015, 26, 2143−2152

work described herein represents the second example of the application of the triazole scan methodology to peptides with biological activities of medicinal interest. In the course of the work, several novel NT-based peptidomimetics with improved metabolic stability and high affinity toward the NTR1 were identified. In particular, the introduction of 1,4-disubstituted, 1,2,3-triazoles as stable *trans* amide bond mimics in the *N*-terminal region of the peptide provided radiolabeled conjugates which exhibited an up to 2-fold improved tumor uptake *in vivo*. The work described herein illustrates the general utility of this novel peptide stabilization approach for the development of peptidomimetics with improved biological properties.

EXPERIMENTAL PROCEDURES

Synthesis and analytical data of Weinreb amides **1a**, **2a**, and **3a** have been published.[41−44] Weinreb amide **4a** was prepared by a procedure reported by Ko et al.[45]

Synthesis of Fmoc-Arg(Boc)$_2$-(NMe)OMe 4a. Fmoc-Arg(Boc)$_2$-OH **4** (400 mg, 0.7 mmol) was dissolved in CH_2Cl_2 (3 mL) and HOBt (100 mg, 0.74 mmol, 1.1 equiv) and EDC (154.1 mg, 0.8 mmol, 1.2 equiv) were added. The reaction mixture was stirred at 0 °C for 15 min and *N*,*O*-dimethylhydroxylamine (47.1 mg, 0.74 mmol, 1.1 equiv) and *N*-methylmorpholine (89 μL, 0.8 mmol, 1.2 equiv) were added. The reaction mixture was stirred for 12 h at rt. The solvent was then removed *in vacuo*, and the resulting residue was partitioned between EtOAc and 1 M aq HCl. The organic layer was separated and washed with 1 M aq HCl (1 × 15 mL), a saturated solution of aq $NaHCO_3$ (1 × 15 mL) and brine (1 × 15 mL), and dried over Mg_2SO_4. After filtration, the solvent was removed *in vacuo*, and the residue was purified by flash chromatography on silica gel (EtOAc/hexane, 3:7) yielding compound **4a** as white crystals (180 mg, 41%). $[\alpha]_D^{20}$ + 3.6 (c = 1.2, $CHCl_3$) ^{1}H NMR (500 MHz, CD_3CN): δ = 11.65 (s, 1H), 8.22 (s, 1H), 7.84−7.82 (dd, *J* = 7.5 Hz, J= 1.3 Hz, 2H), 7.69−7.65 (t, *J* = 7.5 Hz, 2H), 7.43−7.40 (t, *J* = 7.5 Hz, 2H), 7.35−7.31 (tt, *J* = 7.5 Hz, J= 1.3 Hz, 2H), 5.98 (d, *J* = 9.0 Hz, 1H), 4.58 (m, 1H), 4.35−4.29 (m, 1H), 4.23 (t, *J* = 7.0 Hz, 2H), 3.73 (s, 3H), 3.37−3.31 (m, 2H), 3.13 (s, 3H), 1.71−1.54 (m, 4H), 1.48 (s, 9H), 1.42 (s, 9H) ppm. ^{13}C NMR (100 MHz, $CDCl_3$): δ= 164.7, 157.2, 153.9, 145.1, 142.1, 128.6, 128.1, 126.2, 120.9, 84.0, 79.4, 67.1, 51.9, 48.0, 40.8, 29.7, 28.4, 26.1, 26.1 ppm (four ^{13}C signals were not observed presumably due to overlapping signals). ESI-HRMS: [M + H]+ *m*/*z* calcd for $C_{33}H_{46}N_5O_8$: 640.3346, found: 640.3344.

α-Amino alkynes **1c** and **2c** have also been reported. They were synthesized following the general protocol for the synthesis of α-amino alkynes from Boc-protected Weinreb amides (see Supporting Information).[29] CuAAC alkyne substrates **3b** and **4b** have been prepared according to the following procedure for the synthesis of α-amino alkynes from Fmoc-protected Weinreb amides.[24,29]

Synthesis of α-Amino Alkynes from Fmoc-Protected Weinreb Amides. The corresponding Weinreb amide (0.1 mmol) was placed under argon in a flame-dried flask and dissolved in anhydrous CH_2Cl_2 (0.1 M). The solution was cooled to −78 °C (dry ice/diethyl ether bath). 1 M DIBAL-H in toluene (0.3 mL, 0.3 mmol, 3.0 equiv) was added slowly. After 1 h of stirring, the reaction was checked for completion by TLC. If the reaction was not finished, additional 1 M DIBAL-H in toluene (0.1 mL, 0.1 mmol, 1.0 equiv) was added, and the reaction was stirred again for 1 h at −78 °C. After the consumption of the Weinreb amide starting material, the reaction was allowed to warm to −10 °C (ice/NaCl bath), and excess hydride was quenched by the slow addition of anhydrous MeOH (1 mL). K_2CO_3 (414 mg, 0.3 mmol, 3.0 equiv), dimethyl-(1-diazo-2-oxopropyl)phosphonate (300 μL, 0.2 mmol, 2.0 equiv), and MeOH (1 mL) were added at 0 °C, and the reaction mixture was stirred overnight at rt. A saturated solution of Rochelle's salt (potassium sodium tartrate, 5 mL) was added, and after 1 h of stirring at rt, the solution was diluted with water and CH_2Cl_2. The organic phase was separated and the aqueous phase extracted again with CH_2Cl_2 (3 × 30 mL). The combined organic phases were dried over Na_2SO_4 and filtered, and the solvent was removed *in vacuo*. If cleavage of the Fmoc protective group was observed on TLC (ninhydrin-test positive start spots), the crude mixture was dissolved in CH_2Cl_2 (1 mL), and DIPEA (2.5 equiv) and Fmoc-OSu (2.0 equiv) were added. The reaction mixture was stirred overnight at rt and diluted with CH_2Cl_2 and brine. The aqueous phase was extracted with CH_2Cl_2 (3 × 30 mL). The combined organic phases were dried over Na_2SO_4 and filtered, and the solvent was removed *in vacuo*. The corresponding Weinreb amides were purified by flash chromatography on silica gel.

Fmoc-Tyr(^{t}Bu)-alkyne 3b. Compound **3b** was synthesized from compound **3a** (140 mg, 0.3 mmol,) following the protocol for the synthesis of α-amino alkynes from Fmoc-protected Weinreb amides. Flash chromatography of the crude product (EtOAc/hexane, gradient 5:95 to 8:92) yielded compound **3b** as white crystals (62 mg, 51%). $[\alpha]_D^{20}$ = −7.8 (c = 0.6, $CHCl_3$). ^{1}H NMR (500 MHz, $CDCl_3$): δ = 7.77 (dd, *J* = 7.5 Hz, *J* = 1.0 Hz, 2H), 7.57 (d, *J* = 7.5 Hz, 2H), 7.40 (tq, *J* = 7.5 Hz, *J* = 1.0 Hz, 2H), 7.32 (td, *J* = 7.5 Hz, *J* = 1.0 Hz 2H), 7.12 (d, *J* = 8.0 Hz, 2H), 6.92 (dt, *J* = 8.0 Hz, *J* = 2.5 Hz, 2H), 4.94 (d, *J* = 9.0 Hz, 1H), 4.72 (m, 1H), 4.47−4.36 (m, 2H), 4.21 (t, *J* = 7.5 Hz, 1H), 2.97−2.93 (m, 2H), 2.31 (d, *J* = 2.0 Hz, 1H), 1.33 (s, 9H) ppm. ^{13}C NMR (100 MHz, $CDCl_3$): δ= 154.6, 143.9, 141.5, 130.4, 127.9, 127.2, 125.1, 124.1, 120.1, 82.5, 78.5, 72.6, 67.0, 47.3, 44.4, 40.9, 29.0 ppm (two ^{13}C signals were not observed due to overlapping signals but confirmed by HMQC). ESI-HRMS: $[M + Na]^+$ *m*/*z* calcd for $C_{29}H_{29}NNaO_3$: 462.2045, found: 462.2037.

Fmoc-Arg(Boc)$_2$-alkyne 4b. Compound **4b** was synthesized from compound **4a** (500 mg, 0.8 mmol) following the protocol for the synthesis of α-amino alkynes from Fmoc-protected Weinreb amides. Two flash chromatographies (EtOAc/hexane, 3:7) and (MeOH/CH_2Cl_2, 0:100 to 5:95) yielded compound **4b** as white crystals (100 mg, 22%). $[\alpha]_D^{20}$ = −4.1 (c = 0.5, $CHCl_3$). ^{1}H NMR (500 MHz, CD_3CN): δ= 11.53 (s, 1H), 8.21 (m, 1H), 7.81 (dq, *J* = 7.5 Hz, *J* = 1.0 Hz, 2H), 7.63 (t, *J* = 8.5 Hz, 2H), 7.40 (tt, *J* = 7.5 Hz, *J* = 1.0 Hz, 2H), 7.31 (tt, *J* = 7.5 Hz, *J* = 1.0 Hz, 2H), 6.10 (d, *J* = 8.5 Hz, 1H), 4.37−4.32 (m, 3H, Fmoc), 4.21 (t, *J* = 7.5 Hz, 1H), 3.32−3.31 (m, 2H), 2.54 (d, *J* = 2.0 Hz, 1H) 1.65−1.61 (m, 4H), 1.47 (s, 9H), 1.41 (s, 9H) ppm. ^{13}C NMR (100 MHz, $CDCl_3$): δ = 164.6, 157.2, 153.9, 145.1, 128.6, 128.0, 126.1, 120.9, 83.9, 79.4, 67.1, 48.0, 43.5, 40.7, 33.2, 28.4, 28.1, 26.3 ppm (four ^{13}C signals were not observed due to overlapping signals but confirmed by HMQC and HMBC). ESI-HRMS: $[M + H]^+$ *m*/*z* calcd for $C_{32}H_{41}N_4O_6$: 577.3026, found: 577.3024.

Peptide Synthesis. General Procedure A: Manual Solid Phase Peptide Synthesis. The resin (Leu-preloaded PEG−PS Novasyn resin or, in the case of **NT II**, a rink amide MBHA resin LL; 0.01−0.03 mmol) was swollen in DMF (3 × 3 mL) in a syringe fitted with a polypropylene frit and a Teflon

DOI: 10.1021/acs.bioconjchem.5b00444
Bioconjugate Chem. 2015, 26, 2143−2152

tap. The Fmoc-protected amino acid (0.06 mmol, 2.0 equiv), HATU (0.06 mmol, 2.0 equiv), and DIPEA (0.15 mmol, 5.0 equiv) were added to the resin, and the suspension was shaken for 1.5 h at rt. The solvent was removed by filtration, and the resin was repeatedly washed with DMF and CH_2Cl_2. Completion of the reaction was checked by a Kaiser test and repeated if necessary. Coupling of the spacers Fmoc-PEG_4-OH and the chelator DOTA-(*tris*-^{t}Bu) was performed using the same reaction conditions.

General Procedure B: Fmoc Deprotection on the Resin. Twenty percent piperidine in DMF was added to the resin and was left to react for 3 min. The deprotection agent was then filtered off, and this process was repeated three times. The resin was then washed thoroughly with DMF and CH_2Cl_2. The yield of the deprotection was determined by UV titration (λ = 301 nm) of the fluorenylmethylpiperidine adduct (ε = 7800 mol^{-1} dm^3 cm^{-1}).

General Procedure C: Introduction of the Azido Functionality at the *N*-terminus of the Peptide on the Resin.[31] After Fmoc-cleavage to obtain the free *N*-terminal amine, imidazole-1-sulfonyl azide hydrochloride (5.0 equiv) and DIPEA (6.0 equiv) were added in DMF to the resin. The suspension was shaken for 1 h at rt. The solvent was filtered off, and the resin was washed with DMF and CH_2Cl_2. Completion of the reaction was checked with a Kaiser test and by the colorimetric test for solid-support azides developed by Punna and Finn.[46]

General Procedure D: Solid Phase Copper Catalyzed Cycloaddition (CuAAC). The resin functionalized *N*-terminally with an azide was swollen with anhydrous DMF. The corresponding Fmoc-protected α-amino alkyne (2.0 equiv), DIPEA (1.0 equiv), tetrakis(acetonitrile)copper(I) hexafluorophosphate (0.5 equiv), and TBTA (0.5 equiv) were added in anhydrous DMF. The suspension was shaken for 12−15 h at rt. The resin was then washed repeatedly with a solution of 0.5% diethyldithiocarbamate in DMF. Washing steps were repeated with DMF and CH_2Cl_2. The Kaiser test and azide test were performed to check the completion of the reaction.

General Procedure E: Cleavage and Purification of the Peptide Conjugates. After completion of the elongation of the amino acid sequence and the attachment of the spacer and the chelator, the conjugates were cleaved and deprotected by a standard treatment of 6 h with TFA/H_2O/TIS/PhOH (87.5:5:2.5:2.5). The resin was filtered off, and the cleavage mixture was removed by evaporation with a stream of argon. The crude peptide conjugate was then precipitated by the addition of ice-cold diethyl ether (15 mL). After centrifugation and two washing steps with cold diethyl ether, the peptide conjugate was dissolved in H_2O and acetonitrile (1:1) and purified by preparative HPLC, using 0.1% TFA in H_2O as solvent A and 0.1% TFA in MeCN as solvent B.

Synthesis of DOTA-PEG_4-Arg-Arg-Pro-Tyr-Ile-Leu (NT I). Peptide conjugate **NT I** was prepared following procedures **B**, **D**, and **E** using a Leu-preloaded PEG−PS Novasyn resin (0.03 mmol) and commercial DOTA-(*tris*-^{t}Bu), Fmoc-PEG_4-COOH, Fmoc-Arg(Pbf)-OH, Fmoc-Pro-OH, Fmoc-Tyr(*t*Bu)-OH, and Fmoc-Ile-OH. Purification of the by preparative HPLC (80−70% A in B in 15 min) yielded peptide conjugate **NT I** in high purity (>98%), as a white powder (1 mg, 2%). Analytical HPLC: (90−50% A in B in 20 min), t_r= 8.69 min. ESI-HRMS m/z $[M + 2H^+]^{2+}$ calcd for $C_{65}H_{113}N_{17}O_{20}$: 1451.8348; theor. $[M + 2H^+]^{2+}$, 725.9174; found, 725.9174.

Synthesis of DOTA-PEG_4-Arg-Arg-Pro-Tyr-Ile-Leu-ψ-[Tz]-H (NT II). Peptide conjugate **NT II** was prepared following procedures **B**, **D**, and **E**. For the *C*-terminal introduction of a monosubstituted 1,2,3-triazole, a rink amide MBHA resin LL (100−200 mesh; 0.03 mmol) was used. After deprotection of the resin, its amine functionality was converted into an azide following procedure **C**.[47,48] The triazole was formed following general procedure **D**, using Fmoc-Leu-alkyne.[24] Commercially available Fmoc-Ile-OH, Fmoc-Tyr(*t*Bu)-OH, Fmoc-Pro-OH, Fmoc-Arg(Pbf)-OH, Fmoc-PEG_4-COOH, and DOTA-(*tris*-*t*Bu) were then coupled following general procedure **A**. Peptide conjugate **NT II** was obtained in high purity (>99%) as a white powder after purification by preparative HPLC (80−60% A in B in 20 min) (5.0 mg, 11%). Analytical HPLC: (90−50% A in B in 15 min), t_r = 9.10 min. ESI-HRMS m/z $[M + 2H^+]^{2+}$ calcd for $C_{66}H_{115}N_{20}O_{18}$: 1475.8698; theor. $[M + 2H^+]^{2+}$, 737.4310; found, 737.9230.

Synthesis of DOTA-PEG_4-Arg-Arg-Pro-Tyr-Ile-ψ[Tz]-Leu (NT III). Peptide conjugate **NT III** was prepared following procedures **A**, **B**, **C**, **D**, and **E** using a Leu-preloaded PEG-PS resin (0.03 mmol) and Fmoc-Tyr(^{t}Bu)-OH, Fmoc-Pro-OH, Fmoc-Arg(Pbf)-OH, Fmoc-PEG_4-COOH, and DOTA-(*tris*-^{t}Bu). Alkyne **1c** was used as a triazole precursor. The peptide conjugate was **NT III** obtained as a white powder in high purity (>99%) after purification by preparative HPLC (70−65% A in B in 20 min) (2.0 mg, 5%). Analytical HPLC: (90−50% A in B in 15 min), t_r = 10.14 min. LR ESI-MS m/z $[M + 2H^+]^{2+}$ calcd for $C_{66}H_{113}N_{19}O_{19}$: 1475.8460; theor. $[M + 2H^+]^{2+}$, 737.9; found, 738.3.

Synthesis of DOTA-PEG_4-Arg-Arg-Pro-Tyr-ψ[Tz]-Ile-Leu (NT IV). Peptide conjugate **NT IV** was prepared following procedures **A**, **B**, **C**, **D**, and **E** using a Leu-preloaded PEG-PS resin (0.03 mmol) and Fmoc-Ile-OH, Fmoc-Pro-OH, Fmoc-Arg(Pbf)-OH, Fmoc-PEG_4-COOH and DOTA-(*tris*-^{t}Bu). Alkyne **3b** was used as triazole precursor. Purification by preparative HPLC (80−70% A in B in 20 min) and yielded peptide conjugate **NT IV** in high purity (>99%) as a white powder (14.0 mg, 32%). Analytical HPLC: (90−50% A in B in 15 min), t_r= 9.46 min. ESI-HRMS m/z $[M + 2H^+]^{2+}$ calcd for $C_{66}H_{113}N_{19}O_{19}$: 1475.8460; theor. $[M + 2H^+]^{2+}$, 737.9230; found, 737.9226.

Synthesis of DOTA-PEG_4-Arg-Arg-Pro-ψ[Tz]-Tyr-Ile-Leu (NT V). Peptide conjugate **NT V** was prepared following procedures **A**, **B**, **C**, **D**, and **E** using a Leu-preloaded PEG-PS resin (0.03 mmol) and Fmoc-Ile-OH, Fmoc-Tyr(^{t}Bu)-OH, Fmoc-Arg(Pbf)-OH, Fmoc-PEG_4-COOH, and DOTA-(*tris*-^{t}Bu). Alkyne **2c** was used as a triazole precursor. After purification by preparative HPLC (75−70% A in B in 16 min), peptide conjugate **NT V** was obtained in high purity (>98%) as a white powder (2.7 mg, 27%). Analytical HPLC: (90−50% A in B in 15 min), t_r = 9.73 min. ESI-HRMS m/z $[M + 2H^+]^{2+}$ calcd for $C_{66}H_{113}N_{19}O_{19}$: 1475.8460; theor. $[M + 2H^+]^{2+}$, 737.9230; found, 737.9232.

Synthesis of DOTA-PEG_4-Arg-ψ[Tz]-Arg-Pro-Tyr-Ile-Leu (NT VI). Peptide conjugate **NT VI** was prepared following procedures **A**, **B**, **C**, **D**, and **E** using a Leu-preloaded PEG-PS resin (0.03 mmol) and Fmoc-Ile-OH, Fmoc-Tyr(^{t}Bu)-OH, Fmoc-Pro-OH, Fmoc-Arg(Pbf)-OH, Fmoc-PEG_4-COOH, and DOTA-(*tris*-^{t}Bu). Alkyne **4b** was used as a triazole precursor. After purification by preparative HPLC (80−60% A in B in 20 min), peptide conjugate **NT VI** was obtained in high purity (>99%) as a white powder (6.1 mg, 14%). Analytical HPLC: (90−50% A in B in 15 min), t_r = 9.25 min. ESI-HRMS m/z [M

DOI: 10.1021/acs.bioconjchem.5b00444
Bioconjugate Chem. 2015, 26, 2143−2152

+2H$^+$]$^{2+}$ calcd for $C_{66}H_{113}N_{19}O_{19}$: 1475.8460; theor. [M + 2H$^+$]$^{2+}$, 737.9230; found, 737.9226.

Synthesis of DOTA-PEG$_4$-ψ[Tz]-Arg-Arg-Pro-Tyr-Ile-Leu (NT VII). Peptide conjugate **NT VII** was prepared following procedures **A**, **B**, **C**, **D**, and **E** using a Leu-preloaded PEG-PS resin (0.03 mmol) and Fmoc-Ile-OH, Fmoc-Tyr(^{t}Bu)-OH, Fmoc-Pro-OH, Fmoc-Arg(Pbf)-OH, and DOTA-(*tris*-^{t}Bu). Fmoc-PEG$_4$-alkyne was used as a triazole precursor.[24] Peptide conjugate **NT VII** was obtained as a highly pure (>98%) white powder after purification by preparative HPLC (80−60% A in B in 20 min) (2.0 mg, 5%). Analytical HPLC: (90−50% A in B in 15 min), t_r = 9.23 min. ESI-HRMS *m*/*z* [M + 2H$^+$]$^{2+}$ calcd for $C_{65}H_{111}N_{19}O_{19}$: 1461.8304; theor. [M + 2H$^+$]$^{2+}$, 730.9152; found, 730.9152.

Synthesis of DOTA-PEG$_4$-Arg-Arg-Pro-Tyr-Tle-Leu (NT VIII). Peptide conjugate **NT VIII** was prepared following procedures **A**, **D**, and **E** using a Leu-preloaded PEG-PS resin (0.03 mmol) and Fmoc-Tle-OH, Fmoc-Tyr(^{t}Bu)-OH, Fmoc-Pro-OH, Fmoc-Arg(Pbf)-OH, Fmoc-PEG$_4$-COOH, and DOTA-(*tris*-^{t}Bu). Peptide conjugate **NT VII** was obtained as a highly pure (>99%) white powder after purification by preparative HPLC (80−60% A in B in 20 min) (13.0 mg, 30%). Analytical HPLC: (90−50% A in B in 15 min), t_r = 9.00 min. ESI-HRMS *m*/*z* [M + 2H$^+$]$^{2+}$ calcd for $C_{65}H_{113}N_{17}O_{20}$: 1451.8348; theor. [M + 2H$^+$]$^{2+}$, 725.9174; found, 725.917.

Synthesis of DOTA-PEG$_4$-Arg-ψ[Tz]-Arg-Pro-Tyr-Tle-Leu (NT IX). Peptide conjugate **NT IX** was prepared following procedures **A**, **B**, **C**, **D**, and **E** using a Leu-preloaded PEG-PS resin (0.03 mmol) and Fmoc-Tle-OH, Fmoc-Tyr(^{t}Bu)-OH, Fmoc-Pro-OH, Fmoc-Arg(Pbf)-OH, Fmoc-PEG$_4$-COOH, and DOTA-(*tris*-^{t}Bu). Alkyne **4b** was used as triazole precursor. Peptide conjugate **NT IX** was obtained in high purity (>99%) as a white powder after purification by preparative HPLC (80−60% A in B in 20 min) (7.0 mg, 16%). Analytical HPLC: (90−50% H_2O with 0.1% TFA in 15 min), t_r = 10.13 min. ESI-HRMS *m*/*z* [M + 2H$^+$]$^{2+}$ calcd for $C_{66}H_{113}N_{19}O_{19}$: 1475.8460; theor. [M + 2H$^+$]$^{2+}$, 737.9230; found, 737.9232.

Synthesis of DOTA-PEG$_4$-ψ[Tz]-Arg-Arg-Pro-Tyr-Tle-Leu (NT X). Peptide conjugate **NT X** was prepared following procedures **A**, **B**, **C**, **D**, and **E** using a Leu-preloaded PEG-PS resin (0.03 mmol) and Fmoc-Tle-OH, Fmoc-Tyr(^{t}Bu)-OH, Fmoc-Pro-OH, Fmoc-Arg(Pbf)-OH, and DOTA-(*tris*-^{t}Bu). Fmoc-PEG$_4$-alkyne was used as a triazole precursor.[24] Peptide conjugate **NT X** was obtained in high purity (>98%) as a white powder after purification by preparative HPLC (80−60% A in B in 20 min) (6.9 mg, 16%). Analytical HPLC: (90−50% A in B in 15 min), t_r = 10.18 min. ESI-HRMS *m*/*z* [M + 2H$^+$]$^{2+}$ calcd for $C_{65}H_{111}N_{19}O_{19}$: 1461.8304; theor. [M + 2H$^+$]$^{2+}$, 730.9152; found, 730.9145.

Radiolabeling. NT (8−13) derivatives **NT I-X** were radiolabeled with different specific activities depending on the experiments planned. Peptide conjugates were used as stock solutions of 1 mg/mL in H_2O. Then, 5−10 μg (3.5−6.9 nmol conjugate in 5−10 μL of H_2O) of analogues **NT I-X** were added to 150 μL of NH_4OAc buffer (0.4 M, pH 5.0). [^{177}Lu]$LuCl_3$ (37−150 MBq) were added, and the mixture was heated for 30 min at 100 °C. After the quality control via γ-HPLC, dilutions of the radiolabeled conjugates were prepared depending on the experiment (see Supporting Information). All NT (8−13) analogues [^{177}**Lu**]**-NT I-X** were obtained in radiochemical yields and purities of >95% and with a specific activity ranging from 5 to 43 MBq/nmol (not optimized).

***In Vitro* Evaluation: Stability Studies.** The radiolabeled peptide conjugates [^{177}**Lu**]**-NT I-X** (30 pmol, 1 nM in PBS, approximately 0.7 MBq) were incubated in fresh blood serum (1 mL) at 37 °C. At different time points (1, 5, 10, 20, 30, 40, 60, 120, 240, 360 min, and 24 h) aliquots (100 μL) were taken, and the proteins were precipitated in 200 μL of EtOH and centrifuged (5 min, 5000 rpm). The supernatant was again precipitated with 100 μL of EtOH and centrifuged. The supernatant was diluted with H_2O (1:2) and analyzed with γ-HPLC. The kinetics of the degradation of the peptides was fitted with the equation $A_{(t)} = A_0 \cdot \exp(-\lambda \cdot t)$ using GraphPad Prism 5.0 to obtain values of biological half-lives ($t_{1/2}$).

Cell Culture. Human colorectal adenocarcinoma (HT-29) cells were cultured at 37 °C and 5% CO_2 in Dulbecco's modified Eagle's medium (DMEM, high glucose) containing 10% (v/v) fetal bovine serum, L-glutamine (200 mM), 100 IU mL^{-1} penicillin and 100 μg mL^{-1} streptomycin. The cells were subcultured weekly after detaching them with a commercial solution of trypsin-EDTA (1:250) in PBS. For experiments, 8×10^5 cells/well were seeded the night before, reaching a concentration of approximately 10^6 cells/well on the day of the experiment, which was verified by cell-counting (Neubau chamber).

Cell Internalization Experiments. On the day prior to the experiment, HT-29 cells (1×10^6 cells/well) were placed in six-well plates with cell culture medium (1% FBS) and incubated overnight at 37 °C and 5% CO_2 for allowing the cells to attach. On the day of the experiment, the medium was removed, and fresh medium (1% FBS, 1.3 mL) was added. Radiolabeled conjugates [^{177}**Lu**]**-NT I-X** (2.5 pmol per well, 2.5 pM solution in PBS, approximately 0.01 MBq) were added, and the cells were incubated for different time points (30, 60, 120, and 240 min) in triplicate to allow binding and internalization. Nonspecific receptor binding and internalization were determined by blocking experiments in the presence of a 1000-fold excess of NT (8−13) as a blocking agent (2.5 nmol per well, 2.5 nM solution in H_2O). After each time point, the supernatant was removed, and the cells were washed twice with PBS (1 mL). The combined supernatants represent the free, unbound fraction of radioactivity. Receptor-bound radioactivity was determined by incubating the cells on ice twice for 5 min with an acidic glycine solution (1 mL; 100 nM NaCl, 50 nM glycine, pH 2.8). The internalized fraction was isolated by lysis of the cells with 1 M NaOH (1 mL) for 10 min at 37 °C and 5% CO_2. The wells of the lysed cells were washed twice with 1 mL of 1 M NaOH. The radioactivity of the fractions was measured quantitatively in a gamma counter and calculated as a percentage of applied dosage. Data were fitted by nonlinear regression with GraphPad Prism 5.0 (n = 2−3 in triplicate).

Receptor Saturation Studies. HT-29 cells in six-well plates were prepared as described above. In order to reach receptor saturation, the cells were incubated with increasing concentrations of the peptide conjugates [^{177}**Lu**]**-NT I−VII** (0.1, 0.5, 1, 5, 10, 20, 50, 75, and 100 nM). For peptide conjugates [^{177}**Lu**]**-NT VIII-X** with lower receptor affinities, higher concentrations were used to achieve receptor saturation (0.1, 0.5, 1, 5, 10, 20, 50, 75, 100, 200, 400, 800, 1600, and 3200 nM) (see Supporting Information). Nonspecific binding was determined by blocking experiments using a 1000-fold excess of NT (8−13) solution (2.5 nmol/1 mL per well, corresponding to 2.5 μM). After incubation of 1 h at 37 °C and 5% CO_2, the supernatant was removed, and the cells were washed twice with PBS (1 mL per well). The combined supernatants represent the

DOI: 10.1021/acs.bioconjchem.5b00444
Bioconjugate Chem. 2015, 26, 2143−2152

free, unbound radiopeptide fraction. In order to determine the receptor bound and internalized fraction, the cells were treated with 1 M NaOH (1 mL per well) for 10 min at 37 °C and washed twice with 1 M NaOH (1 mL per well). The free and the receptor bound fractions were measured in a gamma counter for quantification. Dissociation constants (K_D) were calculated from the specific binding data by performing a nonlinear regression using GraphPad Prism 5 (n = 2−3 in triplicate).

***In Vivo* Evaluation.** All animal experiments were conducted in compliance with the Swiss animal protection laws and with the ethical principles and guidelines for scientific animal trials established by the Swiss Academy of Medical Sciences and the Swiss Academy of Natural Sciences. Biodistributions of compounds [^{177}**Lu**]-**NT I**, **VI**, **VII**, **VIII**, and **IX** were performed with female nude Foxn1 nu mice (6−8 week old), bearing HT-29 colon carcinoma cell xenografts. For induction of the xenografts, HT-29 cells in a concentration of 7×10^6 cells/mouse were injected subcutaneously on the right shoulder and allowed to grow for 8 days until reaching a diameter of approximately 0.5 cm. On the day of the experiment, the mouse received the ^{177}Lu-labeled peptide analogues (10 pmol/mouse, 0.5−0.7 MBq/mouse) into the tail vein. Three reference solutions of the radiotracer per time point were prepared and measured in a gamma-counter for quantification of the radioactivity measured in different tissues (% ID/g). The mice were sacrificed at different times (1, 4, 24 h p.i.), and their organs (blood, heart, lungs, liver, spleen, pancreas, stomach, intestine, colon, adrenal, kidneys, muscle, bone, brain, and tumor) were harvested by dissection. The radioactivity in the organs was determined by γ-counting. Three−five animals were used per time point. For blocking experiments, a solution of NT (1−13) (60 nmol/mouse) was coinjected with the radiolabeled compounds. The animals were sacrificed at 1 h p.i. and dissected, and their organs were measured with a γ-counter. Tissue distribution data were calculated as percent injected activity found per gram of tissue (% ID/g; n = 3−5). Statistical analysis was performed with Graphpad Prism 5 using one way ANOVA and Dunnett's multiple test (* $P < 0.05$; ** $P < 0.01$; ***$P < 0.001$). [^{177}**Lu**]-**NT VI** and [^{177}**Lu**]-**NT VII** were compared to reference [^{177}**Lu**]-**NT I** and [^{177}**Lu**]-**NT IX** to reference [^{177}**Lu**]-**NT VIII**.

■ ASSOCIATED CONTENT

Supporting Information

The Supporting Information is available free of charge on the ACS Publications website at DOI: 10.1021/acs.bioconjchem.5b00444.

Analytical data of α-amino alkyne building blocks, nonradiolabeled peptide conjugates, dipeptides for determination of the enantiomeric purity of α-amino alkynes, ^{177}Lu-labeled peptide conjugates (^{1}H/^{13}C NMR, MS, UV-HPLC, γ-HPLC), and detailed results of *in vitro* and *in vivo* experiments (including the data of blocking experiments) (PDF)

■ AUTHOR INFORMATION

Corresponding Author

*Tel: +41 78 707 3616. Fax: +41 61 265 5559. E-mail: t.mindt@gmx.ch.

Notes

The authors declare no competing financial interest.

■ ACKNOWLEDGMENTS

This work was supported by the Swiss National Science Foundation (grants Nr. 205321-132280 and 200020-146385). We thank ITM (Munich, Germany) for the supply of n.c.a. Lu-177 and Rudolf von Wartburg and Nadia Tognoni (University of Basel Hospital, Switzerland) for technical assistance.

■ REFERENCES

(1) Carraway, R., and Leeman, S. E. (1973) Isolation of a New Hypotensive Peptide, Neurotensin, from Bovine Hypothalami. *J. Biol. Chem. 248*, 6854−6861.

(2) Kitabgi, P., Carraway, R., and Leeman, S. E. (1976) Isolation of a Tridecapeptide from Bovine Intestinal Tissue and Its Partial Characterization as Neurotensin. *J. Biol. Chem. 251*, 7053−7058.

(3) Li, J. H., Sicard, F., Salam, M. A., Baek, M., LePrince, J., Vaudry, H., Kim, K., Kwon, H. B., and Seong, J. Y. (2005) Molecular cloning and functional characterization of a type-I neurotensin receptor (NTR) and a novel NTR from the bullfrog brain. *J. Mol. Endocrinol. 34*, 793−807.

(4) Vincent, J. P., Mazella, J., and Kitabgi, P. (1999) Neurotensin and neurotensin receptors. *Trends Pharmacol. Sci. 20*, 302−309.

(5) Reubi, J. C., Waser, B., Schaer, J. C., and Laissue, J. A. (1999) Neurotensin receptors in human neoplasms: High incidence in Ewing's sarcomas. *Int. J. Cancer 82*, 213−218.

(6) Souaze, F., Dupouy, S., Viardot-Foucault, V., Bruyneel, E., Attoub, S., Gespach, C., Gompel, A., and Forgez, P. (2006) Expression of neurotensin and NT1 receptor in human breast cancer: A potential role in tumor progression. *Cancer Res. 66*, 6243−6249.

(7) Reubi, J. C., Waser, B., Friess, H., Buchler, M., and Laissue, J. (1998) Neurotensin receptors: a new marker for human ductal pancreatic adenocarcinoma. *Gut 42*, 546−550.

(8) Granier, C., Vanrietschoten, J., Kitabgi, P., Poustis, C., and Freychet, P. (1982) Synthesis and Characterization of Neurotensin Analogs for Structure Activity Relationship Studies - Acetyl-Neurotensin-(8−13) Is the Shortest Analog with Full Binding and Pharmacological Activities. *Eur. J. Biochem. 124*, 117−125.

(9) Garcia-Garayoa, E., Allemann-Tannahill, L., Blauenstein, P., Willmann, M., Carrel-Remy, N., Tourwe, D., Iterbeke, K., Conrath, P., and Schubiger, P. A. (2001) In vitro and in vivo evaluation of new radiolabeled neurotensin(8−13) analogues with high affinity for NT1 receptors. *Nucl. Med. Biol. 28*, 75−84.

(10) Vincent, B., Vincent, J. P., and Checler, F. (1994) Neurotensin and neuromedin N undergo distinct catabolic processes in murine astrocytes and primary cultured neurons. *Eur. J. Biochem. 221*, 297−306.

(11) Lugrin, D., Vecchini, F., Doulut, S., Rodriguez, M., Martinez, J., and Kitabgi, P. (1991) Reduced Peptide-Bond Pseudopeptide Analogs of Neurotensin - Binding and Biological-Activities, and In Vitro Metabolic Stability. *Eur. J. Pharmacol. 205*, 191−198.

(12) Bruehlmeier, M., Garayoa, E. G., Blanc, A., Holzer, B., Gergely, S., Tourwe, D., Schubiger, P. A., and Blauenstein, P. (2002) Stabilization of neurotensin analogues: effect on peptide catabolism, biodistribution and tumor binding. *Nucl. Med. Biol. 29*, 321−327.

(13) de Visser, M., Janssen, P. J. J. M., Srinivasan, A., Reubi, J. C., Waser, B., Erion, J. L., Schmidt, M. A., Krenning, E. P., and de Jong, M. (2003) Stabilised (^{111})In-labeled DTPA- and DOTA-conjugated neurotensin analogues for imaging and therapy of exocrine pancreatic cancer. *Eur. J. Nucl. Med. Mol. Imaging 30*, 1134−1139.

(14) Kokko, K. P., Hadden, M. K., Orwig, K. S., Mazella, J., and Dix, T. A. (2003) In Vitro Analysis of Stable, Receptor-Selective Neurotensin[8−13] Analogues. *J. Med. Chem. 46*, 4141−4148.

(15) Hultsch, C., Pawelke, B., Bergmann, R., and Wuest, F. (2006) Synthesis and evaluation of novel multimeric neurotensin(8−13) analogs. *Bioorg. Med. Chem. 14*, 5913−5920.

(16) Röhrich, A., Bergmann, R., Kretzschmann, A., Noll, S., Steinbach, J., Pietzsch, J., and Stephan, H. (2011) A novel tetrabranched neurotensin(8−13) cyclam derivative: Synthesis, ^{64}Cu-labeling and biological evaluation. *J. Inorg. Biochem. 105*, 821−832.

DOI: 10.1021/acs.bioconjchem.5b00444
Bioconjugate Chem. 2015, 26, 2143−2152

(17) Buchegger, F., Bonvin, F., Kosinski, M., Schaffland, A. O., Prior, J., Reubi, J. C., Blauenstein, P., Tourwe, D., Garcia Garayoa, E., and Bischof Delaloye, A. (2003) Radiolabeled neurotensin analog, ^{99m}Tc-NT-XI, evaluated in ductal pancreatic adenocarcinoma patients. *J. Nucl. Med. 44*, 1649−1654.
(18) Tornoe, C. W., Christensen, C., and Meldal, M. (2002) Peptidotriazoles on solid phase: [1,2,3]-triazoles by regiospecific copper(I)-catalyzed 1,3-dipolar cycloadditions of terminal alkynes to azides. *J. Org. Chem. 67*, 3057−3064.
(19) Horne, W. S., Yadav, M. K., Stout, C. D., and Ghadiri, M. R. (2004) Heterocyclic peptide backbone modifications in an alpha-helical coiled coil. *J. Am. Chem. Soc. 126*, 15366−15367.
(20) Tischler, M., Nasu, D., Empting, M., Schmelz, S., Heinz, D. W., Rottmann, P., Kolmar, H., Buntkowsky, G., Tietze, D., and Avrutina, O. (2012) Braces for the peptide backbone: insights into structure-activity relationships of protease inhibitor mimics with locked amide conformations. *Angew. Chem., Int. Ed. 51*, 3708−3012.
(21) Angell, Y. L., and Burgess, K. (2007) Peptidomimetics via copper-catalyzed azide-alkyne cycloadditions. *Chem. Soc. Rev. 36*, 1674−1689.
(22) Pedersen, D. S., and Abell, A. (2011) 1,2,3-Triazoles in Peptidomimetic Chemistry. *Eur. J. Org. Chem. 2011*, 2399−2411.
(23) Valverde, I. E., and Mindt, T. L. (2013) 1,2,3-Triazoles as Amide-bond Surrogates in Peptidomimetics. *Chimia 67*, 262−266.
(24) Valverde, I. E., Bauman, A., Kluba, C. A., Vomstein, S., Walter, M. A., and Mindt, T. L. (2013) 1,2,3-Triazoles as Amide Bond Mimics: Triazole Scan Yields Protease-Resistant Peptidomimetics for Tumor Targeting. *Angew. Chem., Int. Ed. 52*, 8957−8960.
(25) Beltramo, M., Robert, V., Galibert, M., Madinier, J. B., Marceau, P., Dardente, H., Decourt, C., De Roux, N., Lomet, D., Delmas, et al. (2015) Rational design of triazololipopeptides analogs of kisspeptin inducing a long-lasting increase of gonadotropins. *J. Med. Chem. 58*, 3459−3470.
(26) Bergmann, R., Scheunemann, M., Heichert, C., Mäding, P., Wittrisch, H., Kretzschmar, M., Rodig, H., Tourwé, D., Iterbeke, K., Chavatte, et al. (2002) Biodistribution and catabolism of ^{18}F-labeled neurotensin(8−13) analogs. *Nucl. Med. Biol. 29*, 61−72.
(27) Dickson, H. D., Smith, S. C., and Hinkle, K. W. (2004) A convenient scalable one-pot conversion of esters and Weinreb amides to terminal alkynes. *Tetrahedron Lett. 45*, 5597−5599.
(28) Muller, S., Liepold, B., Roth, G. J., and Bestmann, H. J. (1996) An improved one-pot procedure for the synthesis of alkynes from aldehydes. *Synlett 1996*, 521−522.
(29) Tischler, M., Nasu, D., Empting, M., Schmelz, S., Heinz, D. W., Rottmann, P., Kolmar, H., Buntkowsky, G., Tietze, D., and Avrutina, O. (2012) Braces for the Peptide Backbone: Insights into Structure-Activity Relationships of Protease Inhibitor Mimics with Locked Amide Conformations. *Angew. Chem., Int. Ed. 51*, 3708−3712.
(30) Goddard-Borger, E. D., and Stick, R. V. (2007) An efficient, inexpensive, and shelf-stable diazotransfer reagent: Imidazole-1-sulfonyl azide hydrochloride. *Org. Lett. 9*, 3797−3800.
(31) Hansen, M. B., van Gurp, T. H. M., van Hest, J. C. M., and Lowik, D. W. P. M. (2012) Simple and Efficient Solid-Phase Preparation of Azido-peptides. *Org. Lett. 14*, 2330−2333.
(32) Rostovtsev, V. V., Green, L. G., Fokin, V. V., and Sharpless, K. B. (2002) A stepwise Huisgen cycloaddition process: Copper(I)-catalyzed regioselective "ligation" of azides and terminal alkynes. *Angew. Chem., Int. Ed. 41*, 2596−2599.
(33) Mascarin, A., Valverde, I. E., and Mindt, T. L. (2013) Effect of a spacer moiety on radiometal labeled Neurotensin derivatives. *Radiochim. Acta 101*, 733−737.
(34) Maes, V., Garcia-Garayoa, E., Blauenstein, P., and Tourwe, D. (2006) Novel Tc-99m-labeled neurotensin analogues with optimized biodistribution properties. *J. Med. Chem. 49*, 1833−1836.
(35) Maschauer, S., Einsiedel, J., Haubner, R., Hocke, C., Ocker, M., Hubner, H., Kuwert, T., Gmeiner, P., and Prante, O. (2010) Labeling and glycosylation of peptides using click chemistry: a general approach to (18)F-glycopeptides as effective imaging probes for positron emission tomography. *Angew. Chem., Int. Ed. 49*, 976−979.
(36) Rosch, F., and Baum, R. P. (2011) Generator-based PET radiopharmaceuticals for molecular imaging of tumors: on the way to THERANOSTICS. *Dalton Trans. 40*, 6104−6111.
(37) Garcia-Garayoa, E., Maes, V., Blauenstein, P., Blanc, A., Hohn, A., Tourwe, D., and Schubiger, P. A. (2006) Double-stabilized neurotensin analogues as potential radiopharmaceuticals for NTR-positive tumors. *Nucl. Med. Biol. 33*, 495−503.
(38) White, J. F., Noinaj, N., Shibata, Y., Love, J., Kloss, B., Xu, F., Gvozdenovic-Jeremic, J., Shah, P., Shiloach, J., Tate, C. G., and Grisshammer, R. (2012) Structure of the agonist-bound neurotensin receptor. *Nature 490*, 508−513.
(39) Henry, J. A., Horwell, D. C., Meecham, K. G., and Rees, D. C. (1993) A structure-affinity study of the amino acid side-chains in neurotensin: N and C terminal deletions and Ala-scan. *Bioorg. Med. Chem. Lett. 3*, 949−952.
(40) Sparr, C., Purkayastha, N., Yoshinari, T., Seebach, D., Maschauer, S., Prante, O., Hübner, H., Gmeiner, P., Kolesinska, B., Cescato, et al. (2013) Syntheses, Receptor Bindings, in vitro and in vivo Stabilities and Biodistributions of DOTA-Neurotensin(8−13) Derivatives Containing β-Amino Acid Residues − A Lesson about the Importance of Animal Experiments. *Chem. Biodiversity 10*, 2101−2121.
(41) Ko, E. W., and Burgess, K. (2011) Pyrrole-Based Scaffolds for Turn Mimics. *Org. Lett. 13*, 980−983.
(42) Fehrentz, J.-A., and Castro, B. (1983) An Efficient Synthesis of Optically Active α-(t-Butoxycarbonylamino)-aldehydes from α-Amino Acids. *Synthesis 1983*, 676−678.
(43) Woo, J. C. S., Fenster, E., and Dake, G. R. (2004) A convenient method for the conversion of hindered carboxylic acids to N-methoxy-N-methyl (Weinreb) amides. *J. Org. Chem. 69*, 8984−8986.
(44) Iera, J. A., Appella, D. H., Jenkins, L. M. M., Kajiyama, H., and Kopp, J. B. (2010) Solid-phase synthesis and screening of N-acylated polyamine (NAPA) combinatorial libraries for protein binding. *Bioorg. Med. Chem. Lett. 20*, 6500−6503.
(45) Ko, E., Liu, J., Perez, L. M., Lu, G., Schaefer, A., and Burgess, K. (2011) Universal peptidomimetics. *J. Am. Chem. Soc. 133*, 462−477.
(46) Punna, S., and Finn, M. G. (2004) A convenient colorimetric test for aliphatic azides. *Synlett*, 99−100.
(47) Harju, K., Vahermo, M., Mutikainen, I., and Yli-Kauhaluoma, J. (2003) Solid-phase synthesis of 1,2,3-triazoles via 1,3-dipolar cycloaddition. *J. Comb. Chem. 5*, 826−833.
(48) Cohrt, A. E., Jensen, J. F., and Nielsen, T. E. (2010) Traceless azido linker for the solid-phase synthesis of NH-1,2,3-triazoles via Cu-catalyzed azide-alkyne cycloaddition reactions. *Org. Lett. 12*, 5414−5417.
(49) Valverde I. E., Vomstein S., Fischer C. A, Mascarin A., and Mindt.T. L. (2015) Probing the Backbone Function of Tumor Targeting Peptides by an Amide-to-Triazole Substitution Strategy. *J. Med. Chem.* DOI: 10.1021/acs.jmedchem.5b00994.

DOI: 10.1021/acs.bioconjchem.5b00444
Bioconjugate Chem. 2015, 26, 2143−2152